

Measurement of the Relative Branching Fractions for $B^- \rightarrow D/D^*/D^{**}(D^{(*)}\pi)\ell^-\bar{\nu}_\ell$ with a Large Sample of Tagged B Mesons

The BABAR Collaboration

July 27, 2006

Abstract

We present a study of B semileptonic decays into charm final states based on 211.7 fb^{-1} of data collected at the $\Upsilon(4S)$ resonance with the BABAR detector at the PEP-II e^+e^- storage ring. Using a novel technique based on the simultaneous fit of a set of variables reconstructed on the recoil of a B tagged in an hadronic decay mode, we measure the relative branching fractions $\Gamma(B^- \rightarrow D^0\ell^-\bar{\nu}_\ell)/\Gamma(B^- \rightarrow DX\ell^-\bar{\nu}_\ell) = 0.210 \pm 0.017 \text{ (stat.)} \pm 0.021 \text{ (syst.)}$, $\Gamma(B^- \rightarrow D^{*0}\ell^-\bar{\nu}_\ell)/\Gamma(B^- \rightarrow DX\ell^-\bar{\nu}_\ell) = 0.611 \pm 0.022 \text{ (stat.)} \pm 0.027 \text{ (syst.)}$ and $\Gamma(B^- \rightarrow D^{**0}(D^{(*)}\pi)\ell^-\bar{\nu}_\ell)/\Gamma(B^- \rightarrow DX\ell^-\bar{\nu}_\ell) = 0.173 \pm 0.017 \text{ (stat.)} \pm 0.021 \text{ (syst.)}$.

Submitted to the 33rd International Conference on High-Energy Physics, ICHEP 06,
26 July—2 August 2006, Moscow, Russia.

Stanford Linear Accelerator Center, Stanford University, Stanford, CA 94309

Work supported in part by Department of Energy contract DE-AC02-76SF00515.

The *BABAR* Collaboration,

B. Aubert, R. Barate, M. Bona, D. Boutigny, F. Couderc, Y. Karyotakis, J. P. Lees, V. Poireau,
V. Tisserand, A. Zghiche

*Laboratoire de Physique des Particules, IN2P3/CNRS et Université de Savoie, F-74941 Annecy-Le-Vieux,
France*

E. Grauges

Universitat de Barcelona, Facultat de Física, Departament ECM, E-08028 Barcelona, Spain

A. Palano

Università di Bari, Dipartimento di Fisica and INFN, I-70126 Bari, Italy

J. C. Chen, N. D. Qi, G. Rong, P. Wang, Y. S. Zhu

Institute of High Energy Physics, Beijing 100039, China

G. Eigen, I. Ofte, B. Stugu

University of Bergen, Institute of Physics, N-5007 Bergen, Norway

G. S. Abrams, M. Battaglia, D. N. Brown, J. Button-Shafer, R. N. Cahn, E. Charles, M. S. Gill,
Y. Groysman, R. G. Jacobsen, J. A. Kadyk, L. T. Kerth, Yu. G. Kolomensky, G. Kukartsev,
D. Lopes Pegna, G. Lynch, L. M. Mir, T. J. Orimoto, M. Pripstein, N. A. Roe, M. T. Ronan, W. A. Wenzel
Lawrence Berkeley National Laboratory and University of California, Berkeley, California 94720, USA

P. del Amo Sanchez, M. Barrett, K. E. Ford, A. J. Hart, T. J. Harrison, C. M. Hawkes, S. E. Morgan,
A. T. Watson

University of Birmingham, Birmingham, B15 2TT, United Kingdom

T. Held, H. Koch, B. Lewandowski, M. Pelizaeus, K. Peters, T. Schroeder, M. Steinke

Ruhr Universität Bochum, Institut für Experimentalphysik 1, D-44780 Bochum, Germany

J. T. Boyd, J. P. Burke, W. N. Cottingham, D. Walker

University of Bristol, Bristol BS8 1TL, United Kingdom

D. J. Asgeirsson, T. Cuhadar-Donszelmann, B. G. Fulsom, C. Hearty, N. S. Knecht, T. S. Mattison,
J. A. McKenna

University of British Columbia, Vancouver, British Columbia, Canada V6T 1Z1

A. Khan, P. Kyberd, M. Saleem, D. J. Sherwood, L. Teodorescu

Brunel University, Uxbridge, Middlesex UB8 3PH, United Kingdom

V. E. Blinov, A. D. Bukin, V. P. Druzhinin, V. B. Golubev, A. P. Onuchin, S. I. Serednyakov,
Yu. I. Skovpen, E. P. Solodov, K. Yu Todyshev

Budker Institute of Nuclear Physics, Novosibirsk 630090, Russia

D. S. Best, M. Bondioli, M. Bruinsma, M. Chao, S. Curry, I. Eschrich, D. Kirkby, A. J. Lankford, P. Lund,
M. Mandelkern, R. K. Mommsen, W. Roethel, D. P. Stoker

University of California at Irvine, Irvine, California 92697, USA

S. Abachi, C. Buchanan

University of California at Los Angeles, Los Angeles, California 90024, USA

S. D. Foulkes, J. W. Gary, O. Long, B. C. Shen, K. Wang, L. Zhang
University of California at Riverside, Riverside, California 92521, USA

H. K. Hadavand, E. J. Hill, H. P. Paar, S. Rahatlou, V. Sharma
University of California at San Diego, La Jolla, California 92093, USA

J. W. Berryhill, C. Campagnari, A. Cunha, B. Dahmes, T. M. Hong, D. Kovalskyi, J. D. Richman
University of California at Santa Barbara, Santa Barbara, California 93106, USA

T. W. Beck, A. M. Eisner, C. J. Flacco, C. A. Heusch, J. Kroseberg, W. S. Lockman, G. Nesom, T. Schalk,
B. A. Schumm, A. Seiden, P. Spradlin, D. C. Williams, M. G. Wilson
University of California at Santa Cruz, Institute for Particle Physics, Santa Cruz, California 95064, USA

J. Albert, E. Chen, A. Dvoretzkii, F. Fang, D. G. Hitlin, I. Narsky, T. Piatenko, F. C. Porter, A. Ryd,
A. Samuel
California Institute of Technology, Pasadena, California 91125, USA

G. Mancinelli, B. T. Meadows, K. Mishra, M. D. Sokoloff
University of Cincinnati, Cincinnati, Ohio 45221, USA

F. Blanc, P. C. Bloom, S. Chen, W. T. Ford, J. F. Hirschauer, A. Kreisel, M. Nagel, U. Nauenberg,
A. Olivas, W. O. Ruddick, J. G. Smith, K. A. Ulmer, S. R. Wagner, J. Zhang
University of Colorado, Boulder, Colorado 80309, USA

A. Chen, E. A. Eckhart, A. Soffer, W. H. Toki, R. J. Wilson, F. Winklmeier, Q. Zeng
Colorado State University, Fort Collins, Colorado 80523, USA

D. D. Altenburg, E. Feltresi, A. Hauke, H. Jasper, J. Merkel, A. Petzold, B. Spaan
Universität Dortmund, Institut für Physik, D-44221 Dortmund, Germany

T. Brandt, V. Klose, H. M. Lacker, W. F. Mader, R. Nogowski, J. Schubert, K. R. Schubert, R. Schwierz,
J. E. Sundermann, A. Volk
Technische Universität Dresden, Institut für Kern- und Teilchenphysik, D-01062 Dresden, Germany

D. Bernard, G. R. Bonneaud, E. Latour, Ch. Thiebaux, M. Verderi
Laboratoire Leprince-Ringuet, CNRS/IN2P3, Ecole Polytechnique, F-91128 Palaiseau, France

P. J. Clark, W. Gradl, F. Muheim, S. Playfer, A. I. Robertson, Y. Xie
University of Edinburgh, Edinburgh EH9 3JZ, United Kingdom

M. Andreotti, D. Bettoni, C. Bozzi, R. Calabrese, G. Cibinetto, E. Luppi, M. Negrini, A. Petrella,
L. Piemontese, E. Prencipe
Università di Ferrara, Dipartimento di Fisica and INFN, I-44100 Ferrara, Italy

F. Anulli, R. Baldini-Ferrolì, A. Calcaterra, R. de Sangro, G. Finocchiaro, S. Pacetti, P. Patteri,
I. M. Peruzzi,¹ M. Piccolo, M. Rama, A. Zallo
Laboratori Nazionali di Frascati dell'INFN, I-00044 Frascati, Italy

¹Also with Università di Perugia, Dipartimento di Fisica, Perugia, Italy

A. Buzzo, R. Capra, R. Contri, M. Lo Vetere, M. M. Macri, M. R. Monge, S. Passaggio, C. Patrignani,
E. Robutti, A. Santroni, S. Tosi

Università di Genova, Dipartimento di Fisica and INFN, I-16146 Genova, Italy

G. Brandenburg, K. S. Chaisanguanthum, M. Morii, J. Wu
Harvard University, Cambridge, Massachusetts 02138, USA

R. S. Dubitzky, J. Marks, S. Schenk, U. Uwer
Universität Heidelberg, Physikalisches Institut, Philosophenweg 12, D-69120 Heidelberg, Germany

D. J. Bard, W. Bhimji, D. A. Bowerman, P. D. Dauncey, U. Egede, R. L. Flack, J. A. Nash,
M. B. Nikolich, W. Panduro Vazquez
Imperial College London, London, SW7 2AZ, United Kingdom

P. K. Behera, X. Chai, M. J. Charles, U. Mallik, N. T. Meyer, V. Ziegler
University of Iowa, Iowa City, Iowa 52242, USA

J. Cochran, H. B. Crawley, L. Dong, V. Eyges, W. T. Meyer, S. Prell, E. I. Rosenberg, A. E. Rubin
Iowa State University, Ames, Iowa 50011-3160, USA

A. V. Gritsan
Johns Hopkins University, Baltimore, Maryland 21218, USA

A. G. Denig, M. Fritsch, G. Schott
Universität Karlsruhe, Institut für Experimentelle Kernphysik, D-76021 Karlsruhe, Germany

N. Arnaud, M. Davier, G. Grosdidier, A. Höcker, F. Le Diberder, V. Lepeltier, A. M. Lutz, A. Oyanguren,
S. Pruvot, S. Rodier, P. Roudeau, M. H. Schune, A. Stocchi, W. F. Wang, G. Wormser
*Laboratoire de l'Accélérateur Linéaire, IN2P3/CNRS et Université Paris-Sud 11, Centre Scientifique
d'Orsay, B.P. 34, F-91898 ORSAY Cedex, France*

C. H. Cheng, D. J. Lange, D. M. Wright
Lawrence Livermore National Laboratory, Livermore, California 94550, USA

C. A. Chavez, I. J. Forster, J. R. Fry, E. Gabathuler, R. Gamet, K. A. George, D. E. Hutchcroft,
D. J. Payne, K. C. Schofield, C. Touramanis
University of Liverpool, Liverpool L69 7ZE, United Kingdom

A. J. Bevan, F. Di Lodovico, W. Menges, R. Sacco
Queen Mary, University of London, E1 4NS, United Kingdom

G. Cowan, H. U. Flaecher, D. A. Hopkins, P. S. Jackson, T. R. McMahon, S. Ricciardi, F. Salvatore,
A. C. Wren
*University of London, Royal Holloway and Bedford New College, Egham, Surrey TW20 0EX, United
Kingdom*

D. N. Brown, C. L. Davis
University of Louisville, Louisville, Kentucky 40292, USA

J. Allison, N. R. Barlow, R. J. Barlow, Y. M. Chia, C. L. Edgar, G. D. Lafferty, M. T. Naisbit,
J. C. Williams, J. I. Yi

University of Manchester, Manchester M13 9PL, United Kingdom

C. Chen, W. D. Hulsbergen, A. Jawahery, C. K. Lae, D. A. Roberts, G. Simi

University of Maryland, College Park, Maryland 20742, USA

G. Blaylock, C. Dallapiccola, S. S. Hertzbach, X. Li, T. B. Moore, S. Saremi, H. Staengle

University of Massachusetts, Amherst, Massachusetts 01003, USA

R. Cowan, G. Sciolla, S. J. Sekula, M. Spitznagel, F. Taylor, R. K. Yamamoto

*Massachusetts Institute of Technology, Laboratory for Nuclear Science, Cambridge, Massachusetts 02139,
USA*

H. Kim, S. E. Mclachlin, P. M. Patel, S. H. Robertson

McGill University, Montréal, Québec, Canada H3A 2T8

A. Lazzaro, V. Lombardo, F. Palombo

Università di Milano, Dipartimento di Fisica and INFN, I-20133 Milano, Italy

J. M. Bauer, L. Cremaldi, V. Eschenburg, R. Godang, R. Kroeger, D. A. Sanders, D. J. Summers,
H. W. Zhao

University of Mississippi, University, Mississippi 38677, USA

S. Brunet, D. Côté, M. Simard, P. Taras, F. B. Viaud

Université de Montréal, Physique des Particules, Montréal, Québec, Canada H3C 3J7

H. Nicholson

Mount Holyoke College, South Hadley, Massachusetts 01075, USA

N. Cavallo,² G. De Nardo, F. Fabozzi,³ C. Gatto, L. Lista, D. Monorchio, P. Paolucci, D. Piccolo,
C. Sciacca

Università di Napoli Federico II, Dipartimento di Scienze Fisiche and INFN, I-80126, Napoli, Italy

M. A. Baak, G. Raven, H. L. Snoek

*NIKHEF, National Institute for Nuclear Physics and High Energy Physics, NL-1009 DB Amsterdam, The
Netherlands*

C. P. Jessop, J. M. LoSecco

University of Notre Dame, Notre Dame, Indiana 46556, USA

T. Allmendinger, G. Benelli, L. A. Corwin, K. K. Gan, K. Honscheid, D. Hufnagel, P. D. Jackson,
H. Kagan, R. Kass, A. M. Rahimi, J. J. Regensburger, R. Ter-Antonyan, Q. K. Wong

Ohio State University, Columbus, Ohio 43210, USA

N. L. Blount, J. Brau, R. Frey, O. Igonkina, J. A. Kolb, M. Lu, R. Rahmat, N. B. Sinev, D. Strom,
J. Strube, E. Torrence

University of Oregon, Eugene, Oregon 97403, USA

²Also with Università della Basilicata, Potenza, Italy

³Also with Università della Basilicata, Potenza, Italy

A. Gaz, M. Margoni, M. Morandin, A. Pompili, M. Posocco, M. Rotondo, F. Simonetto, R. Stroili, C. Voci

Università di Padova, Dipartimento di Fisica and INFN, I-35131 Padova, Italy

M. Benayoun, H. Briand, J. Chauveau, P. David, L. Del Buono, Ch. de la Vaissière, O. Hamon,
B. L. Hartfiel, M. J. J. John, Ph. Leruste, J. Malcès, J. Ocariz, L. Roos, G. Therin

*Laboratoire de Physique Nucléaire et de Hautes Energies, IN2P3/CNRS, Université Pierre et Marie
Curie-Paris6, Université Denis Diderot-Paris7, F-75252 Paris, France*

L. Gladney, J. Panetta

University of Pennsylvania, Philadelphia, Pennsylvania 19104, USA

M. Biasini, R. Covarelli

Università di Perugia, Dipartimento di Fisica and INFN, I-06100 Perugia, Italy

C. Angelini, G. Batignani, S. Bettarini, F. Bucci, G. Calderini, M. Carpinelli, R. Cenci, F. Forti,
M. A. Giorgi, A. Lusiani, G. Marchiori, M. A. Mazur, M. Morganti, N. Neri, E. Paoloni, G. Rizzo,
J. J. Walsh

Università di Pisa, Dipartimento di Fisica, Scuola Normale Superiore and INFN, I-56127 Pisa, Italy

M. Haire, D. Judd, D. E. Wagoner

Prairie View A&M University, Prairie View, Texas 77446, USA

J. Biesiada, N. Danielson, P. Elmer, Y. P. Lau, C. Lu, J. Olsen, A. J. S. Smith, A. V. Telnov

Princeton University, Princeton, New Jersey 08544, USA

F. Bellini, G. Cavoto, A. D’Orazio, D. del Re, E. Di Marco, R. Faccini, F. Ferrarotto, F. Ferroni,
M. Gaspero, L. Li Gioi, M. A. Mazzoni, S. Morganti, G. Piredda, F. Polci, F. Safai Tehrani, C. Voena

Università di Roma La Sapienza, Dipartimento di Fisica and INFN, I-00185 Roma, Italy

M. Ebert, H. Schröder, R. Waldi

Universität Rostock, D-18051 Rostock, Germany

T. Adye, N. De Groot, B. Franek, E. O. Olaiya, F. F. Wilson

Rutherford Appleton Laboratory, Chilton, Didcot, Oxon, OX11 0QX, United Kingdom

R. Aleksan, S. Emery, A. Gaidot, S. F. Ganzhur, G. Hamel de Monchenault, W. Kozanecki, M. Legendre,
G. Vasseur, Ch. Yèche, M. Zito

DSM/Dapnia, CEA/Saclay, F-91191 Gif-sur-Yvette, France

X. R. Chen, H. Liu, W. Park, M. V. Purohit, J. R. Wilson

University of South Carolina, Columbia, South Carolina 29208, USA

M. T. Allen, D. Aston, R. Bartoldus, P. Bechtle, N. Berger, R. Claus, J. P. Coleman, M. R. Convery,
M. Cristinziani, J. C. Dingfelder, J. Dorfan, G. P. Dubois-Felsmann, D. Dujmic, W. Dunwoodie,
R. C. Field, T. Glanzman, S. J. Gowdy, M. T. Graham, P. Grenier,⁴ V. Halyo, C. Hast, T. Hryn’ova,
W. R. Innes, M. H. Kelsey, P. Kim, D. W. G. S. Leith, S. Li, S. Luitz, V. Luth, H. L. Lynch,
D. B. MacFarlane, H. Marsiske, R. Messner, D. R. Muller, C. P. O’Grady, V. E. Ozcan, A. Perazzo,
M. Perl, T. Pulliam, B. N. Ratcliff, A. Roodman, A. A. Salnikov, R. H. Schindler, J. Schwiening,
A. Snyder, J. Stelzer, D. Su, M. K. Sullivan, K. Suzuki, S. K. Swain, J. M. Thompson, J. Va’vra, N. van

⁴Also at Laboratoire de Physique Corpusculaire, Clermont-Ferrand, France

Bakel, M. Weaver, A. J. R. Weinstein, W. J. Wisniewski, M. Wittgen, D. H. Wright, A. K. Yarritu, K. Yi,
C. C. Young

Stanford Linear Accelerator Center, Stanford, California 94309, USA

P. R. Burchat, A. J. Edwards, S. A. Majewski, B. A. Petersen, C. Roat, L. Wilden

Stanford University, Stanford, California 94305-4060, USA

S. Ahmed, M. S. Alam, R. Bula, J. A. Ernst, V. Jain, B. Pan, M. A. Saeed, F. R. Wappler, S. B. Zain

State University of New York, Albany, New York 12222, USA

W. Bugg, M. Krishnamurthy, S. M. Spanier

University of Tennessee, Knoxville, Tennessee 37996, USA

R. Eckmann, J. L. Ritchie, A. Satpathy, C. J. Schilling, R. F. Schwitters

University of Texas at Austin, Austin, Texas 78712, USA

J. M. Izen, X. C. Lou, S. Ye

University of Texas at Dallas, Richardson, Texas 75083, USA

F. Bianchi, F. Gallo, D. Gamba

Università di Torino, Dipartimento di Fisica Sperimentale and INFN, I-10125 Torino, Italy

M. Bomben, L. Bosisio, C. Cartaro, F. Cossutti, G. Della Ricca, S. Dittongo, L. Lanceri, L. Vitale

Università di Trieste, Dipartimento di Fisica and INFN, I-34127 Trieste, Italy

V. Azzolini, N. Lopez-March, F. Martinez-Vidal

IFIC, Universitat de Valencia-CSIC, E-46071 Valencia, Spain

Sw. Banerjee, B. Bhuyan, C. M. Brown, D. Fortin, K. Hamano, R. Kowalewski, I. M. Nugent, J. M. Roney,
R. J. Sobie

University of Victoria, Victoria, British Columbia, Canada V8W 3P6

J. J. Back, P. F. Harrison, T. E. Latham, G. B. Mohanty, M. Pappagallo

Department of Physics, University of Warwick, Coventry CV4 7AL, United Kingdom

H. R. Band, X. Chen, B. Cheng, S. Dasu, M. Datta, K. T. Flood, J. J. Hollar, P. E. Kutter, B. Mellado,
A. Mihalyi, Y. Pan, M. Pierini, R. Prepost, S. L. Wu, Z. Yu

University of Wisconsin, Madison, Wisconsin 53706, USA

H. Neal

Yale University, New Haven, Connecticut 06511, USA

1 Introduction

The determination of the individual exclusive branching fractions of $B \rightarrow X_c \ell \bar{\nu}_\ell$ decays⁵ is important for the study of the dynamics of semileptonic decays of the B meson. Precise data on the spectroscopy of the hadronic system is needed to be compared with theoretical predictions, obtained under different assumptions [1, 2, 3, 4]. This is especially important since the mass of the hadronic system, recoiling against the leptonic pair in the decay, is a crucial parameter in the extraction of $|V_{cb}|$ in exclusive semileptonic decays, in isolating $B \rightarrow X_u \ell \bar{\nu}_\ell$ from $B \rightarrow X_c \ell \bar{\nu}_\ell$ decays for determining $|V_{ub}|$, and also in the extraction of the heavy quark masses and other non-perturbative Operator Product Expansion parameters from the distribution of spectral moments in semileptonic decays. This is exemplified by the fact that one of the leading sources of systematic uncertainty in the extraction of $|V_{cb}|$ from the exclusive decay $\bar{B} \rightarrow D^* \ell \bar{\nu}_\ell$ is our limited knowledge of the background due to $\bar{B} \rightarrow D^* \pi \ell \bar{\nu}_\ell$ [5]. Reducing this uncertainty is of crucial importance, as lattice calculations promise to improve the theoretical accuracy on the form factor normalization to 2-3 %. Improvements in our knowledge of $B \rightarrow X_c \ell \bar{\nu}_\ell$ decays will also benefit the accuracy in the extraction of $|V_{ub}|$, as analyses are extending their probe into kinematical regions where these decays represent a sizable background.

The first determination of the fractions of D^{**} states in semileptonic b decays was obtained by the ALEPH [6], DELPHI [7, 8] and OPAL [9] experiments at LEP, where some information on the mass distributions of these states was also extracted, and by CLEO [10] at CESR. In particular, the kinematics at LEP, where the B hadrons had a significant boost and were separated in opposite hemispheres, allowed analyses based on the topology of the particle tracks with respect to the decay vertices. On the other hand, primary fragmentation particles represented a background and statistics were limited. More recently, new results have been obtained by the D0 [11] experiment at the Tevatron.

Not only are the data samples at the B factories much larger than those obtained at earlier collider experiments, in addition the feasibility to fully reconstruct one of the two B mesons produced exclusively in the decay of the $\Upsilon(4S)$ resonance permits the study of semileptonic decays of the other B meson in an almost unbiased way. This allows the study of exclusive semileptonic B decays involving charm mesons, specifically D , D^* , resonant D^{**} and non-resonant $D^{(*)}\pi$ with the BABAR data.

Measurements of the largest B meson branching fraction, $\mathcal{B}(\bar{B}^0 \rightarrow D^{*-} \ell^+ \nu_\ell)$, by the CLEO, the LEP and the BABAR and BELLE experiments, based on different reconstruction techniques, need to be reconciled. The current average value [12] has a $\chi^2/\text{ndof} = 14.8/7$ with a probability of just 3.8 %.

Furthermore, there have been so far only very few studies of semileptonic decays to D^{**} and non-resonant final states at the B -factories. BELLE has recently reported the determination of the $D^{(*)}\pi \ell \bar{\nu}_\ell$ decay branching fraction [13].

This study uses a novel technique to extract the exclusive branching fractions⁶ for $B^- \rightarrow D^0 \ell^- \bar{\nu}_\ell$, $B^- \rightarrow D^{*0} \ell^- \bar{\nu}_\ell$ and $B^- \rightarrow D^{**0} \ell^- \bar{\nu}_\ell$ ($\ell = e$ or μ), where D^{**0} denotes here an hadronic final state containing a charm meson and with total mass above that of the D^* state, therefore including both D^{**0} mesons and non-resonant $D^{(*)}\pi$ states.

⁵Here X_c refers to any charm state, X_u to any charmless particle.

⁶Charge-conjugate modes are implied throughout this paper, unless explicitly stated otherwise.

2 The *BABAR* Detector and Dataset

This analysis is based on data collected with the *BABAR* detector at the PEP-II storage ring. The total integrated luminosity of the data set is 211.7 fb^{-1} collected on the $\Upsilon(4S)$. The corresponding number of produced $B\bar{B}$ pairs is 239 million. The *BABAR* detector is described in detail elsewhere [14]. Charged-particle trajectories are measured by a 5-layer double-sided silicon vertex tracker (SVT) and a 40-layer drift chamber (DCH), both operating in a 1.5-T solenoidal magnetic field. Charged-particle identification is provided by the average energy loss (dE/dx) in the tracking devices and by an internally reflecting ring-imaging Cherenkov detector. Photons are detected by a CsI(Tl) electromagnetic calorimeter. Muons are identified by the instrumented magnetic-flux return (IFR). We use Monte Carlo simulations of the *BABAR* detector based on **GEANT** [15] to validate the event reconstruction and the fitting technique used to extract the individual semileptonic branching fractions.

3 Overview of the Analysis Method

The technique developed for this analysis identifies a set of variables, which can be used to discriminate between the individual semileptonic decay modes. These variables are i) the missing mass squared reconstructed with respect to the $D\ell$ system, m_{miss}^2 , ii) the lepton momentum in the B rest frame and iii) the number of reconstructed tracks in addition to those used for reconstructing the D state and the lepton. In order to reduce the sensitivity to Monte Carlo modelling, shapes of the discriminating variables for the D^0 , D^{*0} and D^{**0} decays are extracted from data samples that are highly enriched with the individual decay modes.

Semileptonic B decays containing one fully reconstructed D meson and recoiling against a fully reconstructed B in hadronic decay modes (B_{tag}) are selected. We reconstruct B_{tag} decays of the type $B \rightarrow \bar{D}Y$, where D refers to a charm meson, and Y represents a collection of hadrons with a total charge of ± 1 , composed of $n_1\pi^\pm + n_2K^\pm + n_3K_S^0 + n_4\pi^0$, where $n_1 + n_2 < 6$, $n_3 < 3$, and $n_4 < 3$. Using D^0 and D^{*0} as seeds for B^- decays, we reconstruct about 1000 different decay chains. The kinematic consistency of a B_{tag} candidate with a B meson decay is checked using two variables, the beam-energy substituted mass $m_{ES} = \sqrt{s/4 - \vec{p}_B^2}$ and the energy difference, $\Delta E = E_B - \sqrt{s}/2$. Here \sqrt{s} refers to the total energy, and \vec{p}_B and E_B denote the momentum and energy of the B_{tag} candidate in the $\Upsilon(4S)$ center of mass frame. For correctly identified B_{tag} , the m_{ES} distribution peaks at the B meson mass, while ΔE is consistent with zero. The signal region for tagging B candidates is defined as $m_{ES} > 5.27 \text{ GeV}/c^2$.

The analysis exploits the presence of two charmed mesons in the final state: one used as a seed for the exclusive reconstruction of the B_{tag} , and another in the B semileptonic decay, to obtain a high reconstruction efficiency. The reconstruction starts from the B semileptonic decay, identifying a charm meson of the correct charge-flavor correlation with a lepton with momentum in the $\Upsilon(4S)$ frame higher than $0.6 \text{ GeV}/c$ and then selects the B_{tag} with the smallest ΔE among those which do not overlap with the reconstructed charm meson associated with the lepton. D^0 candidates are reconstructed in nine decay modes: $D^0 \rightarrow K^-\pi^+$, $K^-\pi^+\pi^0$, $K^-\pi^+\pi^+\pi^-$, $K_S^0\pi^+\pi^-$, $K_S^0\pi^+\pi^-\pi^0$, $K_S^0\pi^0$, K^+K^- , $\pi^+\pi^-$, $K_S^0K_S^0$. D^+ candidates are reconstructed in seven decay modes: $D^+ \rightarrow K^-\pi^+\pi^+$, $K^-\pi^+\pi^+\pi^0$, $K_S^0\pi^+$, $K_S^0\pi^+\pi^0$, $K^+K^-\pi^+$, $K_S^0K^+$, $K_S^0\pi^+\pi^+\pi^-$.

This procedure is designed to maximize the efficiency of the $D\ell$ reconstruction and, as a result, the B_{tag} sample shows high purity, without need of further cuts.

Then, $B^- \rightarrow DX\ell^-\bar{\nu}_\ell$ events, where X can be either nothing or any particle(s) from a charged

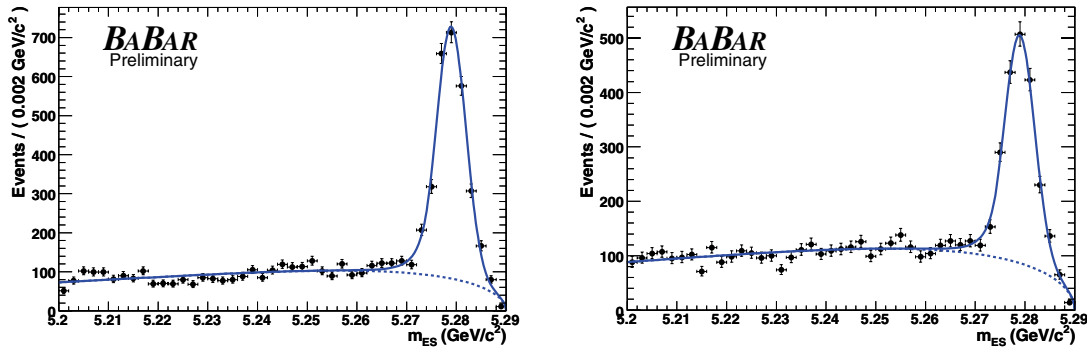


Figure 1: The m_{ES} distributions (data points with statistical errors) for the hadronic B_{tag} with $B^- \rightarrow DXe^- \bar{\nu}_e$ (left) and $B^- \rightarrow DX\mu^- \bar{\nu}_\mu$ (right) events. The solid line represents a fit to the total distribution, the dotted line the combinatorial background. The fitted signal yields are respectively 2409 ± 122 and 1624 ± 130 for the electron and muon samples.

B semileptonic decay into an higher mass charm state (or a non resonant state), are identified by relatively loose selection criteria: we require the charm meson ground state invariant masses M_{D^0} and M_{D^+} to be in the range $1.85 < M_{D^0} < 1.88 \text{ GeV}/c^2$ and $1.853 < M_{D^+} < 1.883 \text{ GeV}/c^2$ and the cosine of the angle between the D candidate and the lepton in the $\Upsilon(4S)$ frame to be less than zero, to reduce background from non B semileptonic decays. After these loose selection criteria, the sample contains leptons from prompt and cascade B meson decays (i.e. the lepton does not come directly from the B) plus various background sources (e.g. photon conversions and π^0 Dalitz decays, combinatoric $B\bar{B}$ background) that need to be subtracted. The contamination from cascade B meson decays (about 15% of the total sample) is removed by using the simulated Monte Carlo distributions for these backgrounds. These events are reweighted to account for possible differences between the branching fractions used in our Monte Carlo simulation and the latest experimental measurements. The photon conversion and π^0 Dalitz decay background (less than 2% of the total electron sample) is removed by using a dedicated algorithm, which performs the reconstruction of vertices between tracks of opposite charge whose invariant mass is compatible with a photon conversion or a π^0 Dalitz decay.

Figure 1 shows the m_{ES} distribution for the B_{tag} candidates in the $B^- \rightarrow DX\ell^- \bar{\nu}_\ell$ sample. We fit this distribution with empirical functions: a Crystal Ball [16] for the signal and an ARGUS function [17] for the background. Combinatoric $B\bar{B}$ background is removed by performing a sideband subtraction by scaling the number of background events in the B_{tag} m_{ES} sideband region $5.21 < m_{ES} < 5.26 \text{ GeV}/c^2$ to the integral of the background function in the signal region. Cross-feed effects (B_{tag}^- candidates erroneously reconstructed as a neutral B) are corrected for using Monte Carlo simulation. We estimate the fraction of \bar{B}^0 events in the reconstructed B^- sample to be 7%.

To determine the total reconstruction efficiencies for individual signal decays using Monte Carlo simulation, the fitted yield of events in the m_{ES} distribution of the B_{tag} decays is compared to the produced number of semileptonic decays in tagged events.

The inclusive distributions of the discriminating variables are determined for the selected $B^- \rightarrow DX\ell^- \bar{\nu}_\ell$ samples. The missing mass squared in the event is defined as:

$$m_{miss}^2 = (p(\Upsilon) - p(B_{tag}) - p(D^{0,+}) - p(\ell))^2 \quad (1)$$

in terms of the various particle four-momenta and for correctly measured signal events it corresponds to the invariant mass of the $X\nu_\ell$ system in the $B^- \rightarrow D^{0,+}X\ell^-\bar{\nu}_\ell$ decay. Thus for $B^- \rightarrow D^0\ell^-\bar{\nu}_\ell$ decays, the missing mass squared corresponds to the neutrino mass and peaks at zero. For semileptonic decays to excited D mesons or non-resonant states, the distribution is shifted towards higher masses. The selection of fully reconstructed events results in an excellent missing mass resolution of $0.04 \text{ GeV}^2/c^4$, an order of magnitude lower compared to non-tagged analyses [18].

The lepton momentum in the $\Upsilon(4S)$ frame is the second variable which can be used to some extent to discriminate among the different B semileptonic decays. Leptons directly produced from B decays will have momenta greater than secondary cascade decays of the type $B \rightarrow D \rightarrow \ell$. For true B semileptonic decays, the lepton momentum is peaked between 1.5 and 2 GeV/c . Leptons from $B \rightarrow D\ell\nu_\ell$ will usually have lower momenta than $B \rightarrow D^*\ell\nu_\ell$, because for $\vec{p}_D \rightarrow 0$, the decay $B \rightarrow D\ell\nu_\ell$ is suppressed, so D mesons will have higher momenta. Leptons from $B \rightarrow D^{**}(D^*)\ell\nu_\ell$ will have much lower momenta, due to the reduced phase space available.

The multiplicity of reconstructed charged tracks in the event, in excess of those accounted for the B_{tag} recoil side, the lepton and the $D^{0,+}$, offers as the missing mass a very high discriminating power to separate the different B semileptonic decays. Every charged track is required to have its point of closest approach to the interaction point less than 10 cm along the beam axis and less than 1.5 cm transverse to the beam axis. The number of additional tracks should be zero for pure $B \rightarrow D^{0,+}\ell\nu_\ell$ decays and larger than zero for those decays involving heavier charm states, provided these decay into a lighter D accompanied by charged particles.

Figure 2 shows the reconstructed missing mass squared, lepton momentum and additional charged track multiplicity distributions for a Monte Carlo sample of $B^- \rightarrow DX\ell^-\bar{\nu}_\ell$ events. The different shapes of the $B^- \rightarrow D^{(*,**)0}\ell^-\bar{\nu}_\ell$ components are clearly visible. As it can be observed, a fraction of $B^- \rightarrow D^{(*)0}\ell^-\bar{\nu}_\ell$ events shows a multiplicity of additional charged tracks greater than zero, coming from badly reconstructed tracks not used for the B_{tag} reconstruction.

4 Reconstruction of the Exclusive Decays $B^- \rightarrow D^{(*,**)0}\ell^-\bar{\nu}_\ell$

To extract the relative branching ratios of the $B^- \rightarrow D^{(*,**)0}\ell^-\bar{\nu}_\ell$ decays from the inclusive $B^- \rightarrow DX\ell^-\bar{\nu}_\ell$ sample, Probability Density Functions (PDFs) corresponding to the different components present in the inclusive distributions must be built. These PDFs are determined using data sets enriched in the different exclusive $B^- \rightarrow D^{(*,**)0}\ell^-\bar{\nu}_\ell$ decays and then parameterized as analytical functions, with the exception of the charged particle track multiplicities which, owing to their discrete nature, are best described by histograms.

The selection of these enriched samples is optimized in terms of their purity, to introduce minimum biases with respect to the true underlying distributions. Background contributions in the exclusive samples include other B semileptonic decays, where one particle is not reconstructed or erroneously added to the charm meson candidate (feed-down and feed-up). We use a sample of $B^- \rightarrow D^{0,+}X\ell^-\bar{\nu}_\ell$ or $B^- \rightarrow D^{*0,+}X\ell^-\bar{\nu}_\ell$ events to reconstruct the exclusive decays. D^0 and D^+ candidates are selected as above. D^* mesons are reconstructed by combining a D candidate and a pion in the $D^{*+} \rightarrow D^0\pi^+(D^+\pi^0)$ and $D^{*0} \rightarrow D^0\pi^0$ decays. These D^* candidates are required to have a mass difference $\Delta m = m_{D\pi} - m_D$ within $\pm 2, 3, 4 \text{ MeV}/c^2$ of its nominal values for the decays $D^{*+} \rightarrow D^+\pi^0$, $D^{*0} \rightarrow D^0\pi^0$ and $D^{*+} \rightarrow D^0\pi^+$ respectively. For the decays with a photon,

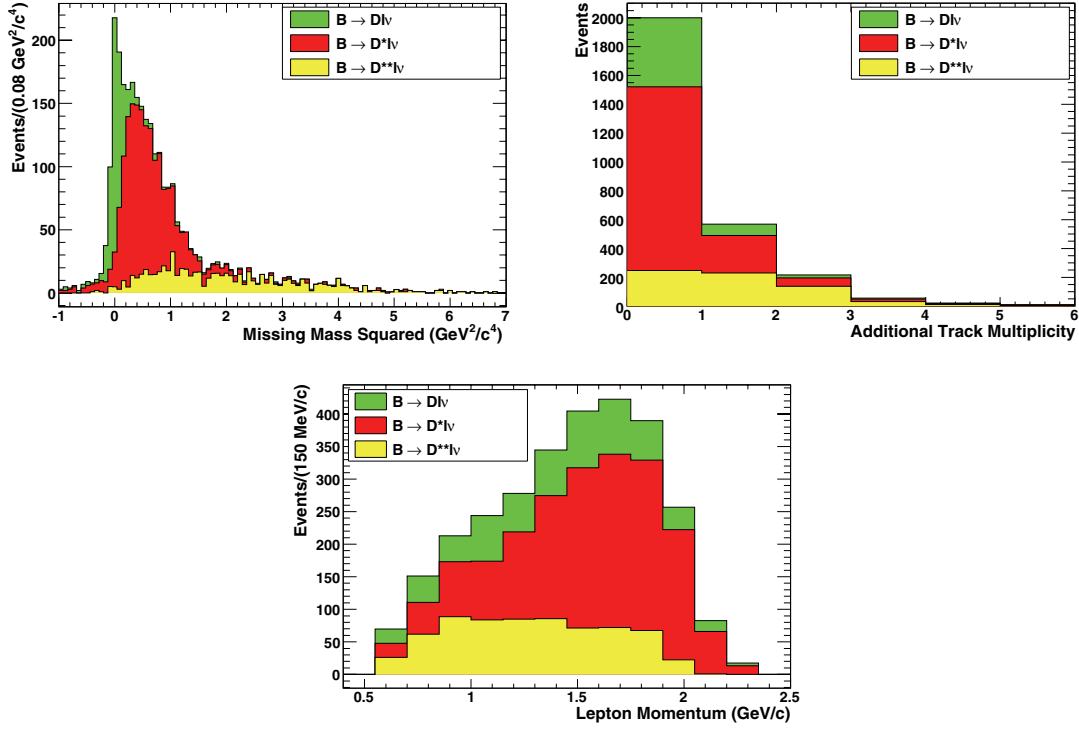


Figure 2: Distributions of the missing mass squared, the multiplicity of additional charged tracks and the lepton momentum spectrum for a Monte Carlo sample of $B^- \rightarrow DX\ell^-\bar{\nu}_\ell$ events used for the relative branching ratio $\Gamma(B^- \rightarrow D^{0,*0},**0\ell^-\bar{\nu}_\ell)/\Gamma(B^- \rightarrow DX\ell^-\bar{\nu}_\ell)$ measurement; the different components are superimposed with different colors.

$D^{*0} \rightarrow D^0\gamma$, we require the mass difference $\Delta m = m_{D\gamma} - m_D$ within ± 9 MeV/ c^2 of its nominal value. D^{**0} states or non resonant $B^- \rightarrow D^{(*)}\pi\ell^-\bar{\nu}_\ell$ decays are reconstructed by combining a D or D^* candidate with a charged pion. Neutral pions are not used at this stage of the reconstruction to avoid large combinatoric background.

Using the four-momentum of the reconstructed $D^{(**)}$ candidate, we compute the corresponding missing mass squared $m_{miss,D^{(**)}}^2$ in the event, defined as:

$$m_{miss,D^{(**)}}^2 = (p(\Upsilon) - p(B_{tag}) - p(D^{(**)}) - p(\ell))^2. \quad (2)$$

For true $B^- \rightarrow D^{(**)0}\ell^-\bar{\nu}_\ell$ semileptonic decays, this missing mass squared will peak at zero. Exclusive samples are then selected by applying the relevant cuts on this variable to select or remove, if we want to eliminate feed-down components, a specific B semileptonic decay.

To select $D^{*0}\ell^-\bar{\nu}_\ell$ decays, the variable $m_{miss,D^{*0}}^2$ is required to be in the range $-0.35 < m_{miss,D^{*0}}^2 < 0.5$ GeV $^2/c^4$, while the unwanted decays are removed, by vetoing the peaking region in the corresponding missing mass squared distribution, i.e. $m_{miss,D^{**+}}^2 > 0.5$ GeV $^2/c^4$ or $m_{miss,D^{**0}}^2 < -0.6$ GeV $^2/c^4$ and $m_{miss,D^{**0}}^2 < -0.2$ GeV $^2/c^4$.

The exclusive decay $B^- \rightarrow D^0\ell^-\bar{\nu}_\ell$ is selected by removing feed-down from D^* and D^{**} events. We require $m_{miss,D^{*0}}^2 < -0.05$ GeV $^2/c^4$ to reduce feed-down from $D^{*0} \rightarrow D^0\gamma$ decays, $m_{miss,D^{*0}}^2 < -0.4$ GeV $^2/c^4$ or $m_{miss,D^{*0}}^2 > 1.0$ GeV $^2/c^4$ for $D^{*0} \rightarrow D^0\pi^0$ decays. Feed-down from D^{*+} events

is reduced by requiring $|m_{miss,D^{*+}}^2| > 0.3 \text{ GeV}^2/c^4$. Feed-down from D^{**} events is reduced by requiring $|m_{miss,D^{**0}}^2| > 0.8 \text{ GeV}^2/c^4$ or $m_{miss,D^{**0}}^2 < -0.5 \text{ GeV}^2/c^4$ for $D^{**0} \rightarrow D^{*+}\pi^-$ and $D^{**0} \rightarrow D^{*0}\pi^0$ decays and $m_{miss,D^{**+}}^2 < -0.5 \text{ GeV}^2/c^4$ for D^{**+} events.

Exclusive $B^- \rightarrow D^{**0}\ell^-\bar{\nu}_\ell$ events are selected by requiring $-0.25 < m_{miss,D^{**+}}^2 < 0.85(0.25) \text{ GeV}^2/c^4$ for $D^{**0} \rightarrow D^+(D^{*+})\pi^-$ decays.

Non B semileptonic decay background and combinatoric $B\bar{B}$ background are subtracted as in the inclusive distribution. Table 1 lists the composition of the reconstructed exclusive samples in terms of purity, feed-up(-down) fractions and non B semileptonic background.

Table 1: Purity and feed-down(up) contributions for the reconstructed exclusive decay modes.

Decay Mode	Purity	Feed-up (D)	Feed-up (D^*)	Feed-down (D^*)	Feed-down (D^{**})	background
$B^- \rightarrow D^0\ell^-\bar{\nu}_\ell$	75%	-	-	19.3%	3.6%	2.5%
$B^- \rightarrow D^{*0}\ell^-\bar{\nu}_\ell$	91%	3.7%	-	-	2.8%	2.6%
$B^- \rightarrow D^{**0}(D^{*+}\pi^-)\ell^-\bar{\nu}_\ell$	85%	0.27%	5.5%	-	-	9.4%
$B^- \rightarrow D^{**0}(D^+\pi^-)\ell^-\bar{\nu}_\ell$	85%	1.2%	4.2%	-	-	9.7%

This reconstruction strategy has been validated to assess whether the exclusive selection procedure induces biases on the shapes of the discriminating variables. This has been done by comparing the distribution of these variables using different selection criteria on Monte Carlo simulated events of the different decay modes $B^- \rightarrow D^{(*,**)0}\ell^-\bar{\nu}_\ell$. The agreement of these distributions is good: residual discrepancies are evaluated as systematic effects.

The final step is the determination of the fractions of D^0 , D^{*0} and D^{**0} decays in the selected inclusive semileptonic sample, by a simultaneous χ^2 fit to the missing mass squared, additional charged track multiplicity and lepton momentum distributions where the relative fractions are treated as free parameters together with the parameters describing the shapes of the discriminating variables. The PDFs for the three different fit components are extracted by fitting simultaneously the corresponding exclusive and inclusive reconstructed distributions. The D^0 missing mass squared PDF is the sum of three Gaussians, with independent means and widths, to account for the upper tail, which is mainly due to feed-down from $B^- \rightarrow D^{*0}\ell^-\bar{\nu}_\ell$ decays where the soft pion or the photon from the D^{*0} is missing. The D^{*0} (D^{**0}) missing mass squared PDF is built by the product of a Gaussian (an exponential) with a polynomial function. The three D^0 , D^{*0} and D^{**0} lepton momentum spectra are parameterized by the product of a polynomial and an exponential which describes the low momentum tail of the spectra. Because we do not reconstruct D^{**0} states involving neutral pions, we use the $B^- \rightarrow D^{*0}\ell^-\bar{\nu}_\ell$ additional charged track multiplicity distribution to model $B^- \rightarrow D^{**0}\ell^-\bar{\nu}_\ell$ events, where the D^{**0} decays in neutral pions.

The total PDF used to model the inclusive distribution is obtained by the sum of the three exclusive PDFs, whose relative weights correspond to the relative fractions of D^0 , D^{*0} and D^{**0} decays in the sample. The sum of the relative weights is constrained to be equal to one. This results in a 33-parameter fit which ensures that statistical correlations are properly taken into account and the uncertainties on the exclusive shapes, obtained on much reduced statistics compared to the inclusive sample, are correctly propagated into the statistical uncertainties on the D^0 , D^{*0} and D^{**0} fractions. The fit also takes into account the feed-up and feed-down fractions in the exclusive shapes, obtained from simulation and contributing to the systematic uncertainty.

The fit results for the $B^- \rightarrow DX\ell^-\bar{\nu}_\ell$ are shown in Figure 3 and 4. Figure 3 shows the fit result for the exclusive missing mass squared and lepton momentum distributions, which are used to build the PDF used to fit the corresponding inclusive distributions, shown in Figure 4. The

simultaneous fit has a total $\chi^2/\text{ndof} = 237/205$.

5 Systematic Studies

Different sources of systematic uncertainties have been estimated. These are divided in various categories. Detector related systematics may arise from discrepancies in the simulation modelling of the track reconstruction and efficiency, particle identification and neutral particle reconstruction.

Uncertainties related to the reconstruction of charged tracks are determined by evaluating the fit stability using different track selection criteria and by a toy Monte Carlo study in which we fluctuate the track multiplicity bin content according to the tracking efficiency uncertainty. The systematic error due to the reconstruction of neutral particles is studied by varying the resolution and efficiency to match those found in control samples on data. We estimate the systematic error due to particle identification by varying the electron and muon identification efficiencies by 2% and 3%, respectively. The misidentification probabilities are varied by 15% for both electrons and muons.

Different systematic uncertainties are evaluated for the inclusive and exclusive reconstruction procedure. For the inclusive reconstruction of the $B^- \rightarrow DX\ell^- \bar{\nu}_\ell$ samples, the weighting factors used to subtract B cascade decays are varied within their errors and the differences in the fitted relative branching ratios are included in the systematic uncertainty. We also evaluate systematic effects associated to the misidentification rate and the tracking efficiency of the photon conversion and π^0 Dalitz decay reconstruction algorithm. The uncertainty of the B_{tag} combinatorial background subtraction is estimated by evaluating differences in the shapes of this background in the sideband and in the signal region using Monte Carlo predictions. We also evaluate the dependence of the sideband scaling factors on the lepton momentum. The systematic error due to the uncertainty in the amount of flavor cross-feed is computed by varying its fraction by a conservative 30%. The effect of uncertainty on reconstruction efficiency mostly cancels in the relative branching ratios; the uncertainty due to the finite Monte Carlo statistics and the m_{ES} fit we use to compute the relative reconstruction efficiency is included accordingly in the systematic error evaluation.

For the exclusive reconstruction of $B^- \rightarrow D^{(*,**)0}\ell^- \bar{\nu}_\ell$ decays, systematic uncertainties arise from the evaluation of the purity of each sample and residual biases on the reconstructed distributions due to the selection criteria. Possible mismatching between data and Monte Carlo is accounted for by varying the feed-down and feed-up fractions within their errors and by evaluating as systematic uncertainties differences in the fit results. We also evaluate possible biases due to the use of reconstructed exclusive distributions to build the PDFs by replacing them with Monte Carlo signal distributions and performing the fit using these shapes. A separate systematic uncertainty is computed for the D^{**0} additional track multiplicity distribution by varying the relative ratio of $D^{**0} \rightarrow D^{(*)+}\pi^-$ and $D^{**0} \rightarrow D^{(*)0}\pi^0$ events which is predicted by our Monte Carlo simulation. The uncertainty of the B_{tag} combinatorial background subtraction and the cross-feed correction is computed as for the inclusive reconstruction.

The fit performance has been extensively tested using simulated samples with varying fractions of the different decay modes. These tests show that the procedure adopted in this analysis is able to extract the decay fractions without significant biases; the statistical errors obtained from the fit are corrected according to the results on independent toy Monte Carlo tests and increased by 15(20)% for the $D^{(*)0}(D^{**0})$ component. We evaluated the systematics due to the fit technique by using different parameterizations of the exclusive shapes. Additional cross-checks were made, repeating the simultaneous fit of the exclusive shape parameters and the exclusive yields in different

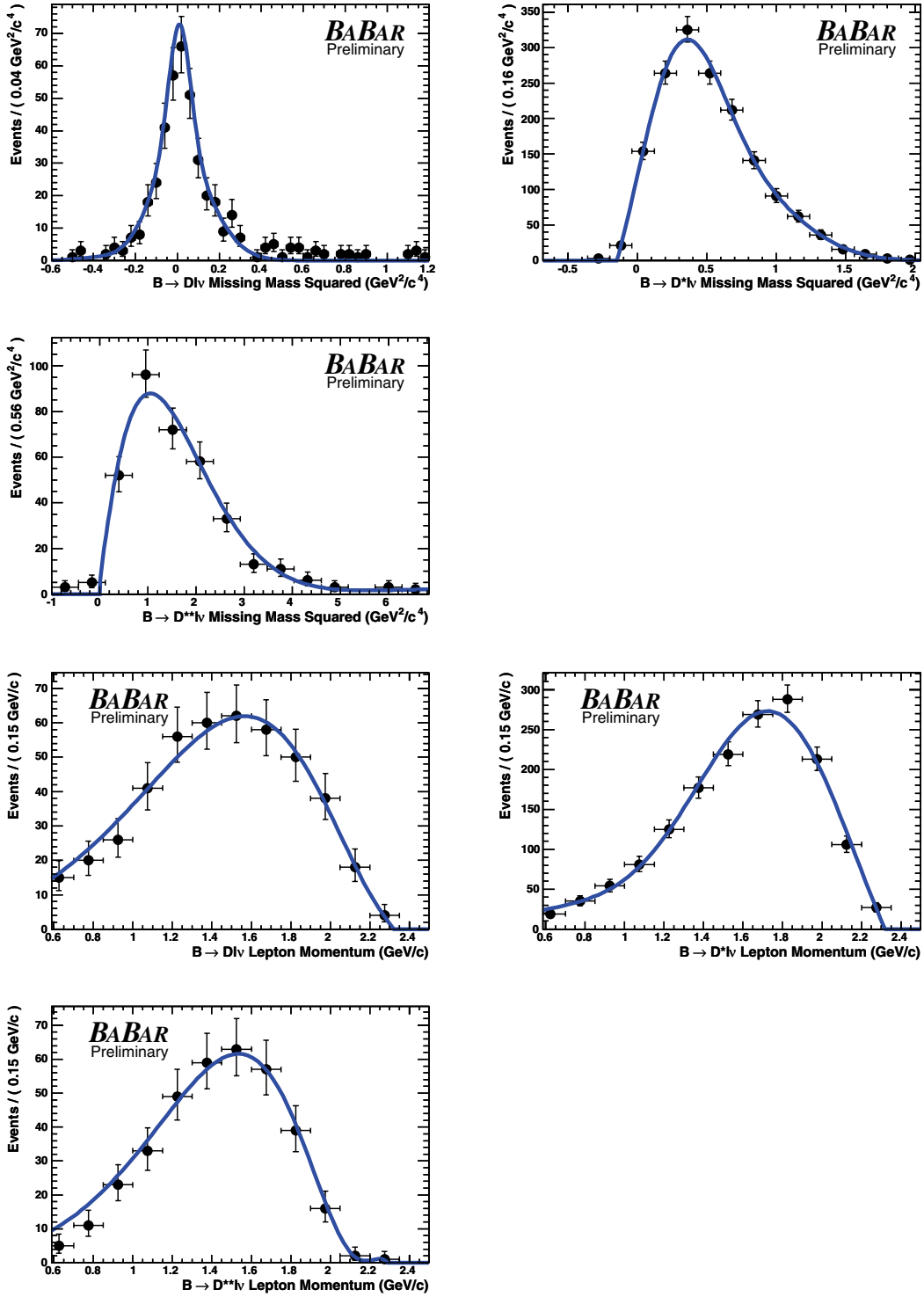


Figure 3: Missing mass squared and lepton momentum distributions for the three selected exclusive decay modes, $B^- \rightarrow D^0 \ell^- \bar{\nu}_\ell$, $B^- \rightarrow D^{*0} \ell^- \bar{\nu}_\ell$ and $B^- \rightarrow D^{**0} \ell^- \bar{\nu}_\ell$. The data are compared to the result of the overall fit (solid line) to the distributions for the selected exclusive and inclusive samples.

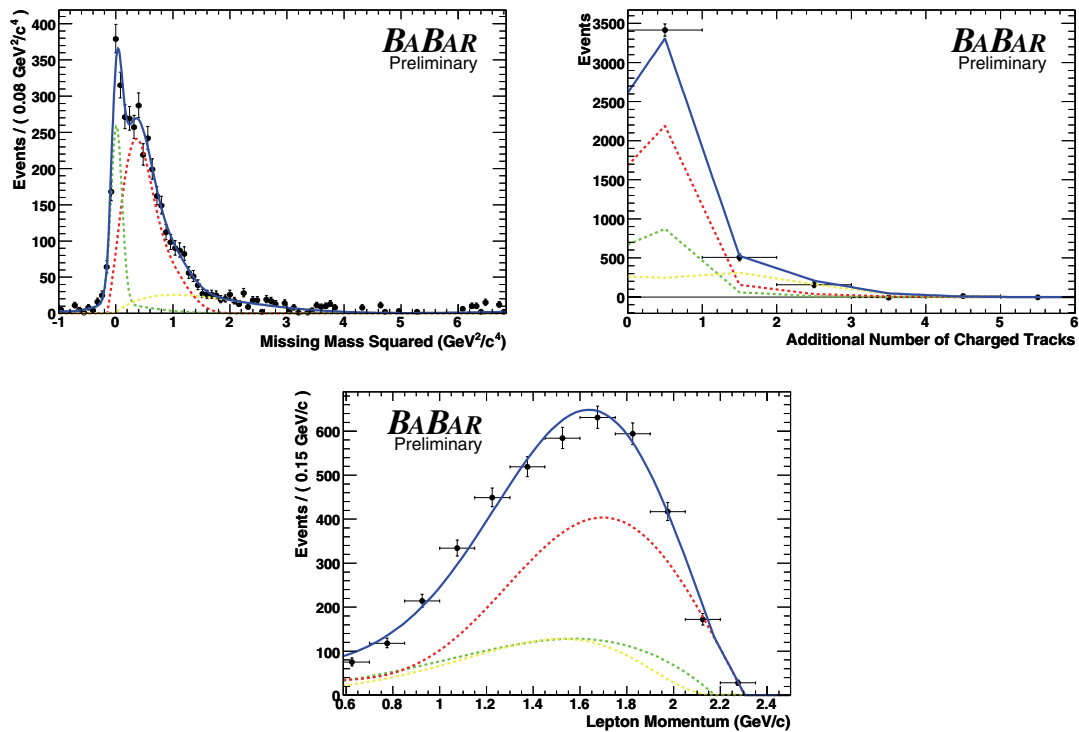


Figure 4: Distributions of the missing mass squared, the multiplicity of additional charged tracks and the lepton momentum spectrum for the selected $B^- \rightarrow DX\ell^-\bar{\nu}_\ell$ events. The data are compared to the results of the overall fit (solid line). The PDFs for the three $D^{(*,**)0}$ components are shown in different colors, from lighter (D^{**0}) to darker (D^{*0}).

configurations, e.g. by fixing the PDF parameters for the exclusive distributions or by only fitting the inclusive distributions.

6 Results

The extraction of the relative fractions of D^0 , D^{*0} and D^{**0} decays in the selected inclusive semileptonic sample gives the relative branching ratios $\Gamma(B^- \rightarrow D^{(*,**)0}\ell^-\bar{\nu}_\ell)/\Gamma(B^- \rightarrow DX\ell^-\bar{\nu}_\ell)$.

The measured branching ratios are reported in Table 2 and the different systematic uncertainties are shown in Table 3.

Table 2: Fitted branching ratios $\Gamma(B^- \rightarrow D^{0,*0,**0}\ell^-\bar{\nu}_\ell)/\Gamma(B^- \rightarrow DX\ell^-\bar{\nu}_\ell)$ with the corresponding statistical uncertainty.

Branching Ratio	Fit Results
$\frac{\Gamma(B^- \rightarrow D^0\ell^-\bar{\nu}_\ell)}{\Gamma(B^- \rightarrow DX\ell^-\bar{\nu}_\ell)}$	$(21.0 \pm 1.44) \%$
$\frac{\Gamma(B^- \rightarrow D^{*0}\ell^-\bar{\nu}_\ell)}{\Gamma(B^- \rightarrow DX\ell^-\bar{\nu}_\ell)}$	$(61.1 \pm 1.94) \%$
$\frac{\Gamma(B^- \rightarrow D^{**0}\ell^-\bar{\nu}_\ell)}{\Gamma(B^- \rightarrow DX\ell^-\bar{\nu}_\ell)}$	$(17.3 \pm 1.44) \%$

Table 3: Systematic uncertainties in the measurement of $\Gamma(B^- \rightarrow D^{(*,**)0}\ell^-\bar{\nu}_\ell)/\Gamma(B^- \rightarrow DX\ell^-\bar{\nu}_\ell)$.

	Systematic uncertainty on $\Gamma(B^- \rightarrow D^{(*,**)0}\ell^-\bar{\nu}_\ell)/\Gamma(B^- \rightarrow DX\ell^-\bar{\nu}_\ell)$		
	$B^- \rightarrow D^0\ell\nu_\ell$	$B^- \rightarrow D^{*0}\ell\nu_\ell$	$B^- \rightarrow D^{**0}\ell\nu_\ell$
Tracking efficiency	0.009	0.008	0.004
Neutral reconstruction	0.001	0.003	0.0009
Electron ID	0.0008	0.002	0.0007
Muon ID	0.006	0.02	0.005
Inclusive Reconstruction			
Cascade decay background	0.01	0.01	0.01
Conversion and Dalitz decay background	0.001	0.004	0.001
MC statistics and M_{ES} fit	0.012	0.01	0.011
Cross-feed corrections	0.001	0.002	0.004
Exclusive Reconstruction			
Feed-down and feed-up corrections	0.003	0.002	0.002
MC signal shapes	0.002	0.002	0.007
D^{**0} track multiplicity	0.005	0.002	0.005
M_{ES} fit	0.0007	0.004	0.003
Cross-feed corrections	0.0003	0.0006	0.0009
Fit Technique			
Missing mass and lepton momentum PDF	0.007	0.002	0.008
Total Systematic Error	0.021	0.027	0.021

No direct measurement of the relative branching ratios $\Gamma(B^- \rightarrow D^{(*,**)0}\ell^-\bar{\nu}_\ell)/\Gamma(B^- \rightarrow DX\ell^-\bar{\nu}_\ell)$ is present in the literature. In the absence of any measurement [5] for B semileptonic decays into charm final states X_c other than D meson states, we can assume the relation:

$$\frac{\Gamma(B^- \rightarrow D^{(*,**)0}\ell^-\bar{\nu}_\ell)}{\Gamma(B^- \rightarrow X_c\ell^-\bar{\nu}_\ell)} = \frac{\Gamma(B^- \rightarrow D^{(*,**)0}\ell^-\bar{\nu}_\ell)}{\Gamma(B^- \rightarrow DX\ell^-\bar{\nu}_\ell)} \quad (3)$$

which can be used with the current best values [12] for $B^- \rightarrow X\ell\nu_\ell$, $b \rightarrow u\ell\nu_\ell$ and the branching fractions $B^- \rightarrow D^{(*,**)0}\ell\bar{\nu}_\ell$ to make a comparison with our results.

The $B^- \rightarrow D^{**0}\ell^-\bar{\nu}_\ell$ component is also sensitive to the presence of $B^- \rightarrow D^{(*)}n\pi\ell^-\bar{\nu}_\ell$ events in the inclusive sample $B^- \rightarrow DX\ell^-\bar{\nu}_\ell$, despite we do not explicitly introduce in the fit the corresponding PDF. By floating its parameters in the fit, the D^{**} PDF can model any excess of events in the inclusive sample $B^- \rightarrow DX\ell^-\bar{\nu}_\ell$, which can be associated to a small $B^- \rightarrow D^{(*)}n\pi\ell^-\bar{\nu}_\ell$ component.

7 Conclusions

Preliminary results of the relative branching fractions of individual semileptonic B decays have been obtained for the B^- decaying into $D^0\ell^-\bar{\nu}_\ell$, $D^{*0}\ell^-\bar{\nu}_\ell$ and $D^{**0}\ell^-\bar{\nu}_\ell$. These measurements are based on a sample of 239 million $\Upsilon(4S) \rightarrow B\bar{B}$ decays collected by the BABAR experiment at the PEP-II asymmetric-energy B factory at SLAC, in events in which one B meson decaying to a hadronic final state is fully reconstructed. A novel technique, based on a multi-parametric fit to a set of discriminating variables in an inclusive sample of $B^- \rightarrow DX\ell^-\bar{\nu}_\ell$ events, has been used to measure the relative branching fractions for $B^- \rightarrow D^0, D^{*0}$ and $D^{**0}(D^{(*)}\pi)\ell^-\bar{\nu}_\ell$ decays. In order to reduce the sensitivity to Monte Carlo modelling, which is especially limited by the poor knowledge of the $B^- \rightarrow D^{**0}(D^{(*)}\pi)\ell^-\bar{\nu}_\ell$ decays, the shapes of the discriminating variables for the D^0, D^{*0} and D^{**0} decays are extracted from selected data samples of exclusive decays.

Correcting the statistical errors as discussed in section 5, we obtain:

$$\begin{aligned} \frac{\Gamma(B^- \rightarrow D^0\ell^-\bar{\nu}_\ell)}{\Gamma(B^- \rightarrow DX\ell^-\bar{\nu}_\ell)} &= 0.210 \pm 0.017 \text{ (stat.)} \pm 0.021 \text{ (syst.)} \\ \frac{\Gamma(B^- \rightarrow D^{*0}\ell^-\bar{\nu}_\ell)}{\Gamma(B^- \rightarrow DX\ell^-\bar{\nu}_\ell)} &= 0.611 \pm 0.022 \text{ (stat.)} \pm 0.027 \text{ (syst.)} \\ \frac{\Gamma(B^- \rightarrow D^{**0}\ell^-\bar{\nu}_\ell)}{\Gamma(B^- \rightarrow DX\ell^-\bar{\nu}_\ell)} &= 0.173 \pm 0.017 \text{ (stat.)} \pm 0.021 \text{ (syst.)} \end{aligned}$$

The BELLE result [13] is consistent with our measurement. The extension of this technique to the $\bar{B}^0 \rightarrow D^{(*,**)0}\ell^-\bar{\nu}_\ell$ decay modes will increase the accuracy of the branching fraction measurements of B semileptonic decay in D meson final states and will help the understanding of the observed difference between the rate for the inclusive semileptonic decay and the sum of the rates for the inclusive modes [5]. Moreover, an accurate measurement of the $B \rightarrow D^{**}\ell\nu$ branching fraction, which is made possible by the use of this method, is important to understand the decay mechanism of this channel, which provides crucial tests of the Heavy Quark Effective Theory and the QCD Sum rules [19].

8 Acknowledgments

We are grateful for the extraordinary contributions of our PEP-II colleagues in achieving the excellent luminosity and machine conditions that have made this work possible. The success of

this project also relies critically on the expertise and dedication of the computing organizations that support *BABAR*. The collaborating institutions wish to thank SLAC for its support and the kind hospitality extended to them. This work is supported by the US Department of Energy and National Science Foundation, the Natural Sciences and Engineering Research Council (Canada), Institute of High Energy Physics (China), the Commissariat à l’Energie Atomique and Institut National de Physique Nucléaire et de Physique des Particules (France), the Bundesministerium für Bildung und Forschung and Deutsche Forschungsgemeinschaft (Germany), the Istituto Nazionale di Fisica Nucleare (Italy), the Foundation for Fundamental Research on Matter (The Netherlands), the Research Council of Norway, the Ministry of Science and Technology of the Russian Federation, and the Particle Physics and Astronomy Research Council (United Kingdom). Individuals have received support from the Marie-Curie IEF program (European Union) and the A. P. Sloan Foundation.

References

- [1] V. Morenas, A. Le Yaouanc, L. Oliver, O. Pene and J. C. Raynal, Phys. Rev. D **56**, 5668 (1997) [arXiv:hep-ph/9706265].
- [2] A. K. Leibovich, Z. Ligeti, I. W. Stewart and M. B. Wise, Phys. Rev. D **57**, 308 (1998) [arXiv:hep-ph/9705467].
- [3] D. Ebert, R. N. Faustov and V. O. Galkin, arXiv:hep-ph/0006187.
- [4] M. Di Pierro and A. K. Leibovich, arXiv:hep-ph/0207134.
- [5] S. Eidelman *et al.* [Particle Data Group], Phys. Lett. B **592** 1 (2004).
- [6] D. Buskulic *et al.* [ALEPH Collaboration], Z. Phys. C **73**, 601 (1997).
- [7] P. Abreu *et al.* [DELPHI Collaboration], Phys. Lett. B **475**, 407 (2000).
- [8] D. Bloch *et al.* [DELPHI Collaboration], DELPHI 2000-106 CONF 405.
- [9] G. Abbiendi *et al.* [OPAL Collaboration], Eur. Phys. J. C **30**, 467 (2003) [arXiv:hep-ex/0301018].
- [10] A. Anastassov *et al.* [CLEO Collaboration], Phys. Rev. Lett. **80**, 4127 (1998) [arXiv:hep-ex/9708035].
- [11] V. M. Abazov *et al.* [D0 Collaboration], Phys. Rev. Lett. **95**, 171803 (2005) [arXiv:hep-ex/0507046].
- [12] Heavy Flavor Averaging Group, <http://www.slac.stanford.edu/xorg/hfag/semi/winter06/winter06.shtml>
- [13] D. Liventsev *et al.* [Belle Collaboration], Phys. Rev. D **72**, 051109 (2005).
- [14] B. Aubert *et al.* [BABAR Collaboration], Nucl. Instrum. Methods A **479**, 1 (2002).
- [15] S. Agostinelli *et al.* [GEANT 4 Collaboration], Nucl. Instrum. Methods A **506**, 250 (2003).
- [16] J. E. Gaiser *et al.*, Phys. Rev. D **34**, 711 (1986).
- [17] H. Albrecht *et al.* (ARGUS Collab.), Z. Phys. C **48**, 543 (1990).

- [18] “Exclusive semileptonic decays of B mesons to D mesons” By ARGUS Collaboration (H. Albrecht et al.). DESY-92-029, Feb 1992.
- [19] A. Le Yaouanc et al., Phys. Lett. B **520**, 25 (2001).